MEASUREMENT OF THE A_2^- MESON MASS SPECTRUM

G. GRAYER, B. HYAMS, C. JONES and P. SCHLEIN *
CERN, Geneva, Switzerland

and

W. BLUM, H. DIETL, W. KOCH, H. LIPPMANN, E. LORENZ, G. LÜTJENS
W. MÄNNER, J. MEISSBURGER, U. STIERLIN and P. WEILHAMMER
Max-Planck-Institut für Physik und Astrophysik, Munich, Germany

Received 12 January 1971

We measure the reaction $\pi^- p \to K^- K_S^0 p$ at 17.2 GeV/c and observe some 1400 $A_2^- \to K^- K_S^0$ decays, with no evidence for a double mass peak. The mass resolution is ±5.7 MeV. The A_2^- is produced in a nearly pure $|j, m> \approx |2,1> + |2,-1>$ state in the Gottfried-Jackson system.

A number of experiments [1-3] observing the A_2 meson have found a double mass peak. Other contradictory results exist [4].

We have studied the A_2 in the reaction

$$\pi^- + p \to K^- + K_S^0 + p \,. \qquad (1)$$

at 17.2 GeV/c incident π^- momentum. This is an "effective-mass" experiment as opposed to previous spark chamber experiments [1-3] which have measured "missing mass". A total of 1934 events of reaction (1) were obtained in the mass range $1000 < M(K^- K_S^0) < 2000$ MeV with a mass resolution of ± 5.7 MeV at the position of the A_2 meson (≈1300 MeV). As in ref. [2], there is very little background below the A_2 in the $K^- K_S^0$ mass spectrum

The apparatus, shown schematically in fig. 1, comprised the following parts for this experiment: a 50 cm long liquid-hydrogen target H_2, traversed by a 17.2 GeV/c π^- beam from the CERN Proton Synchrotron; a spectrometer magnet M with gap 150 cm wide, 50 cm high, and a bending power of 50 kG metres; magnetostrictive wire spark chambers with 24 planes W_1 defining the incident π^- trajectory, 24 planes W_2 recording the trajectories of particles leaving the target, and a further 24 planes W_3 defining the trajectories after the magnet. Sets of scintillation counters S were usie in the trigger logic as follows. A counter hodoscope S_9 consisting of 32, 10 cm wide, vertical scintillator strips served to select a predetermined number of secondary particles. A large threshold Čerenkov counter $\check{C}_2$ detected secondary π mesons with momentum greater than 5 GeV/c. Incident beam particles heavier than π^- were identified by a beam Čerenkov counter $\check{C}_1$.

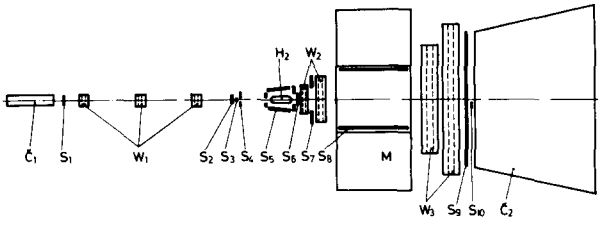

Fig. 1. Schematic layout of apparatus: $\check{C}_1$, $\check{C}_2$ threshold Čerenkov counter; S_1, S_2, S_3, S_4, S_6, S_9, S_{10} scintillation counters; S_5, S_7, S_8 Pb scintillator sandwich counter; W_1, W_2, W_3 spark chambers; H liquid H_2, M magnet.

Two selection modes were used concurrently to trigger the chamber :

Mode 1:

$$[\check{C}_1 S_1 S_2 S_3 \bar{S}_4 (\bar{S}_5)_{\geq 1.5} \bar{S}_7 \bar{S}_8 (S_9)_{=3} \bar{S}_{10}] (\bar{S}_6)_{\geq 2}$$

* Permanent address and support: University of California, Los Angeles, USA. J. S. Guggenheim Fellow (1969-1970).

Mode 2:

$[\check{C}_1 S_1 S_2 S_3 \bar{S}_4 (\bar{S}_5)_{\geq 1.5}$

$\bar{S}_7 \bar{S}_8 (S_9)_{=3} \bar{S}_{10}] (\check{C}_2)_5$ GeV/c π threshold.

Both triggers selected an incident π meson interacting in the hydrogen target, and giving three particles behind the magnet. Events with two or more particles accompanying the $K^- K^0_S$ were rejected by anticoincidence signals from the lead sandwich counters S_5.

In mode 1, K^0_S's decaying after counter S_6 were selected by imposing a pulse-height threshold which rejected events giving more than 1.5 times average ionization in S_6. In mode 2, the counter $\check{C}_2$ was used to rejected any π meson with more than 5 GeV/c momentum. This rejects most peripheral interactions producing pions.

Modes 1 and 2 are complementary in that mode 1 favours fast K^0_S slow K^-, and mode 2 favours K^- slow K^0_S.

With a beam of 4×10^4 π^- these two trigger modes gave 2.5 coincidences per machine pulse. The experiment used about 20% of the spectrometer sensitive timw while running in parallel with triggers for other reactions.

Data processing and event selection. The spark coordinates and counter data of $\approx$ 600 000 triggers were recorded on magnetic tape, and subsequently processed off line.

In order to select the good $K^- K^0_S p$ events, the geometry program demanded

a) three reconstructed secondary trajectories in the spark chambers behind the target;

b) track vertices with topology consistent with reaction (1). For the 12 835 events which survived criteria (a) and (b), the four momenta of all particles were calculated, assigning appropriately $\pi^\pm$ or K^- masses. The remaining sample still contains many events not arising from reaction (1). Reaction (1) is selected with the following additional criteria:

c) only events with a $\pi^+\pi^-$ invariant mass 0.488 GeV $\leq m_{\pi^+\pi^-} \leq$ 0.512 GeV were accepted, leaving 6 837 events. The non-K^0_S background in this interval is about 3%;

d) the missing mass calculated from the four momenta of the incoming pion, the target proton, the K^-, and the K^0_S is shown in fig. 2 for all events fulfilling condition (c). A clear proton peak is seen. We select events with missing mass from 0.3 to 1.25 GeV.

The data have not been constrained by kinematic fits. The $K^- K^0_S$ invariant mass spectrum in the A_2-region is shown in fig. 5. From fig. 2 we estimate that the event samples in fig. 5 contain about 5% background from processes other than $\pi^- p \to K^- K^0_S p$.

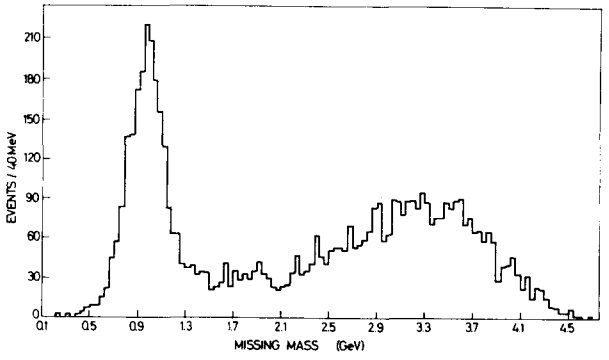

Fig. 2. Missing mass for all events with $0.488 < M(\pi^+\pi^-) < 0.512$ GeV.

Mass resolution. The measured K^0_S mass distribution of the final 1934 event sample (fig.3) has a standard deviation of σ = 4.1 ± 0.1 MeV, which is independent of the K^0_S energy over the range 3 to 14 GeV. We conclude from this fact that our errors are dominated by multiple sacttering. The observed value of σ is in agreement with calculation, based on the amount of scattering material in our spectrometer.

Using the experimental K^0_S width we calculate our resolution for the invariant $K^- K^0_S$ mass at 1300 MeV to be σ = 5.7 ± 0.6 MeV.

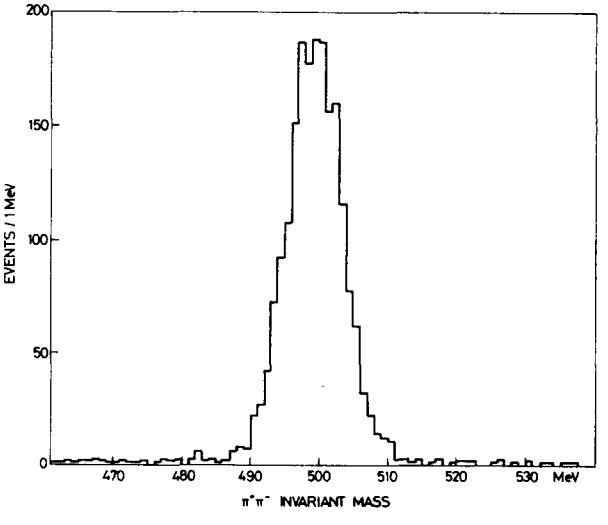

Fig. 3. $\pi^+\pi^-$ invariant mass for events with 0.3 < missing mass < 1.25 GeV.

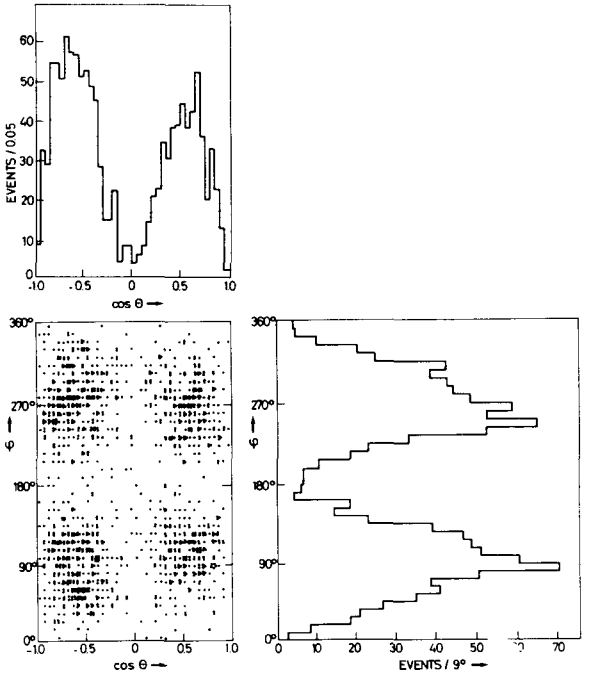

Fig. 4. Scatter plot and projections of K^- angles in Gottfried-Jackson frame, for raw data in the range $1.190 < M(K^-K_S^0) < 1.40$ GeV. The normal to the production plane is beam × A2 .

A sample of $K^- \to \pi^-\pi^-\pi^+$ obtained in a calibration run gave an independent evaluation of our resolution. These events were processed with the same program chain as used for the $K^-K_S^0$ events. We measure $\sigma = 4.0 \pm 0.3$ MeV for the K^- mass which leads to a calculated σ of 5.5 ± 1.0 MeV for the $K^-K_S^0$ mass at 1300 MeV.

From the difference of $+1.6 \pm 0.2$ MeV of our K_S^0 mass from the table value [5] we calculate a systematic shift of $+2.1 \pm 0.5$ MeV for our A_2 mass measurement. We present all data without making any adjustment to our mass scale.

Acceptance and angular distribution of $K^-K_S^0$. The acceptance of the apparatus $A(\theta, \phi)$ (θ, ϕ are defined as K^- angles in the Gottfried-Jackson frame) has been determined in several m and t bins for both triggers by Monte Carlo calculations. In the A_2 region the integrated acceptances (including K_S^0 decay probabilities) are 9.2% and 3.2% with triggers 1 and 2, respectively, for the observed angular distribution.

We have determined the expansion coefficients t_L^M of the acceptance-corrected A_2 decay angular distribution

$$I(\theta, \phi) = \sum_{L,M \geq 0} t_L^M \,\mathrm{Re}\, Y_L^M(\theta, \phi), \quad t_0^0 = \frac{1}{\sqrt{4\pi}}$$

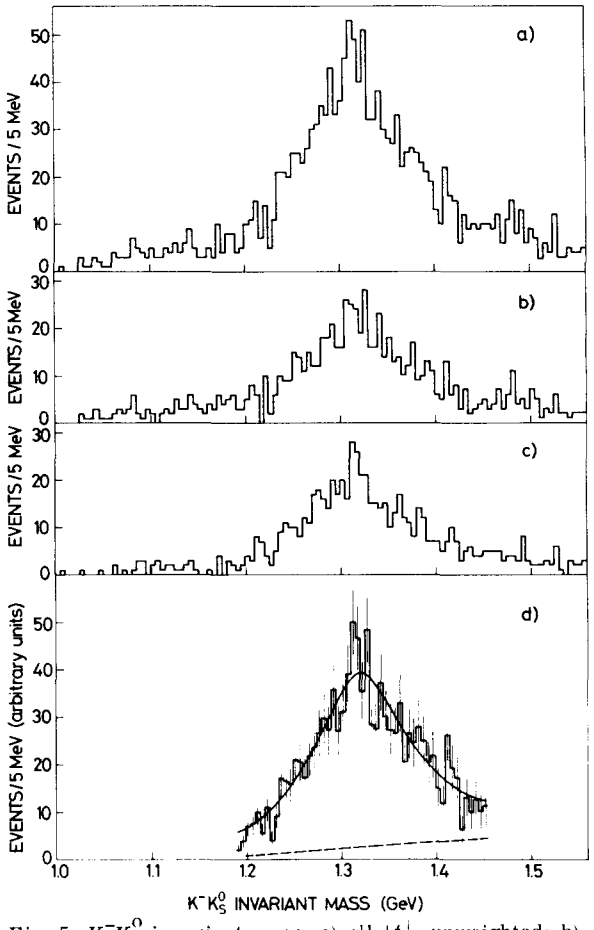

Fig. 5. $K^-K_S^0$ invariant mass: a) all $|t|$, unweighted: b) $|t| < 0.2$, unweighted: c) $0.2 < |t| < 0.7$ $(\mathrm{GeV}/c)^2$, unweighted: d) weighted $0.0 < |t| < 0.7$ $(\mathrm{GeV}/c)^2$. Full line: Breit-Wigner type fit of the form

$$F(m) = \text{linear background} + \frac{2}{\pi} \frac{m - m_0 - \Gamma(m)}{(m^2 - m_0^2)^2 + m^2\Gamma^2_{(m)}}$$

$$\Gamma(m) = \Gamma_0 \left(\frac{q}{q_0}\right)^5 \frac{9 + 3R^2q_0^2 + R^4q_0^4}{9 + 3R^2q^2 + R^4q^4}$$

[6] giving $m_0 = 1321 \pm 3$ MeV and $\Gamma_0 = 123 \pm 7$ MeV with $P_\chi{}^2 = 32\%$. Dashed line: fitted background.

up to $L = M = 6$ for various t and m regions. Only four coefficients are significantly different from 0 in the A_2 peak region, namely t_2^0, t_2^2, t_4^0, t_4^2. Their average values for $1.19 \text{ GeV} < m(K^-K_S^0) < 1.43$ GeV and $0 \leq |t| \leq 0.7$ $(\mathrm{GeV}/c)^2$ are: $t_2^0 = 0.062 \pm 0.013$, $t_2^2 = -0.198 \pm 0.015$, $t_4^0 = -0.155 \pm 0.014$, $t_4^2 = -0.224 \pm 0.022$. These values are very close to those expected (0.090, -0.221, -0.161 and -0.255, respectively) for a pure $|j, m> = |2, 1> + |2, -1>$ state.

The very characteristic structure of the corresponding angular distribution

$$I(\theta, \phi) \propto |Y_{\frac{1}{2}} + Y_{2}^{-1}|^2 \propto \cos^2\theta \sin^2\theta \sin^2\phi \ , \quad (2)$$

may be recognized immediately even in the uncorrected data shown in fig. 4. Because of the complementary nature of the two triggers, the acceptance $A(\theta, \phi)$ does not seriously distort the true (θ, ϕ) distribution. More detailed results about the m and t dependence of the $K^-K^0_S$ angular distribution will be given in a forthcoming paper.

With the $K^-K^0_S$ angular distribution evaluated in the observed m and t range, we have calculated weights to be applied to the observed mass spectrum.

In fig. 5a we plot the unweighted $K^-K^0_S$ mass spectrum in the A_2 mass region in 5 MeV wide bins. Figs. 5b and 5c give the mass spectra for events with the four-momentum transfer t in the intervals $0.0 \leq |t| \leq 0.2$ $(\mathrm{GeV}/c)^2$ and $0.2 \leq |t| \leq 0.7$ $(\mathrm{GeV}/c)^2$. The shape of the mass spectrum is the same in all three histograms.

Fig. 5d shows the weighted mass spectrum for $|t| < 0.7$ $(\mathrm{GeV}/c)^2$. No dip structure can be observed in any one of the above mass spectra. Fitting Breit-Wigner type-formula to the histogram in fig. 5d we get good parametrizations (more than 20% χ^2 probability) of the shape of the mass spectrum. Details of fits to a number of possible resonance forms will be reported later.

Conclusions: 1) The A_2 meson is not a dipole with the parameters suggested in refs. [1, 2]. 2) There is no evidence that the shape of the A_2 mass spectrum depends on t. 3) The A_2 meson has spin 2, and is produced in the state $|2, +1\rangle + |2, -1\rangle$ in the Gottfried-Jackson frame. This may be explained by ρ^0 exchange.

We are indebted to Dr. W. Ochs for useful discussions. We thank our colleagues in the PS Division for providing the excellent pion beam, and the CERN and Garching computing centres for their co-operation.

References

[1] H. Benz et al., Phys. Letters 28B (1968) 233.
[2] R. Baud et al., Phys. Letters 31B (1970) 397.
[3] M. Basile, P. Dalpiaz, P. L. Frabetti, T. Massam, F. Navach, F. L. Navarria, M. A. Schneegans and A. Zichichi, Nuovo Cimento Letters 4 (1970) 838.
[4] A. Barbaro-Galtieri, Experimental meson spectroscopy, eds. C. Baltay and A. H. Rosenfeld (Columbia University Press, 1970) p.331.
[5] Particle Data Group, Phys. Letters 33B (1970) 1.
[6] J. D. Jackson, Nuovo Cimento 34 (1964) 1644.

* * * * *